Supplementary Text S1. **Definition and diagnosis criteria of the 15 included diseases and 15 pathological lesions**.

Diseases

Refractive media opacity

Refractive media opacity is defined as the opacification of the structures of the eye that deflect light, including the cornea, aqueous, crystalline lens, and vitreous[1].

wet Age-related macular degeneration[2]

Age-related macular degeneration (AMD) is an acquired degeneration of the retina that causes significant central visual impairment through a combination of non-neovascular (drusen and retinal pigment epithelium abnormalities), and neovascular derangement (choroidal neovascular membrane formation). AMD is classified into two categories: non-exudative (dry or atrophic) and exudative (wet or neovascular). Critical signs of exudative or neovascular AMD include subretinal choroidal neovascular membrane and other associated manifestations such as RPE detachment or tear, subretinal hemorrhages, subretinal disciform scarring and vitreous hemorrhage.

Branch retinal vein occlusion[3]

Branch retinal vein occlusion (BRVO) is a venous occlusion at any branch of the central retinal vein. BRVO is the most common retinal vein occlusion.

Central retinal vein occlusion[4]

Central retinal vein occlusion is defined as the obstruction of the entire venous outflow from the retina (central retinal vein plus collateral vessels).

Central serous chorioretinopathy[5]

Central serous chorioretinopathy (CSCR) typically occurs in males in their 20s to 50s who exhibit acute or sub-acute central vision loss or distortion. Other common complaints include micropsia, metamorphopsia, hyperopic (most common) or myopic shift, central scotoma, and reduced contrast sensitivity and color saturation[6]. No underlying pathophysiologic mechanisms have been proven, but CSCR is thought to occur due to hyper-permeable choroidal capillaries, which, in association with retinal pigment dysfunction, cause a serous detachment of the neurosensory retina.

Diabetic retinopathy[7]

Diabetic retinopathy represents microvascular end-organ damage as a result of diabetes, with signs of microaneurysms, hemorrhage, hard exudates, cotton wool spots, retinal swelling. It ranges from non-proliferative diabetic retinopathy (NPDR) and its stages to proliferative diabetic retinopathy (PDR).

Epimacular membrane[8]

An epimacular membrane is a fibrocellular tissue found on the inner surface of the macula which is the center of the retina and the region responsible for acute vision.

Macular hole[9]

A macular hole (MH) is a retinal break commonly involving the fovea. Depending on the stage of the MH, a subfoveal lipofuscin-color spot or ring can be noted. In more advanced cases, a partial or full-thickness macular break is observed.

Retinal tears[10]

Retinal tears are full thickness breaks in the neurosensory retina that occur secondary to vitreo-retinal traction, including round holes with operculum and horseshoe tears.

Vitreous hemorrhage[11]

Vitreous hemorrhage is defined as the presence of extravasated blood within the space outlined by the internal limiting membrane of the retina posteriorly and laterally, the nonpigmented epithelium of the

ciliary body laterally and the lens zonular fibers and posterior lens capsule anteriorly.

Retinal detachment[12]

Retinal detachment is defined as the separation of the neurosensory (inner layers) retina from the retinal pigment epithelial layer with a corrugated appearance. A retinal break could be observed in rhegmatogenous retinal detachment.

Optic disc edema[13]

Optic disc edema is the end result of a wide range of pathological processes including nonarteritic anterior ischemic optic neuropathy, retinal vein occlusion and so on.

Optic atrophy[14]

Optic atrophy can occur due to damage within the eye (glaucoma, optic neuritis, papilledema, etc.), along the path of the optic nerve to the brain (tumor, neurodegenerative disorder, trauma, etc.), or it can be congenital (Leber's hereditary optic atrophy, autosomal dominant optic atrophy). Optic atrophy refers to the death of the retinal ganglion cell axons that comprise the optic nerve with the resulting picture of a pale optic nerve on fundoscopy.

Suspected glaucoma

Suspected glaucoma is defined as patients with an increased cup-to-disc ratio over 0.3 in this study. They need to go for more examinations to ensure the diagnosis of glaucoma since an increased cup-to-disc ratio could be physiologic or pathologic[15].

Pathological lesions

Choroidal neovascularization[16]

Choroidal neovascularization (CNV) is part of the spectrum of exudative age-related macular degeneration that consists of an abnormal growth of vessels from the choroidal vasculature to the neurosensory retina through the Bruch's membrane. CNV can also develop in a number of other conditions such as myopic degeneration, chronic central serous chorioretinopathy, macular telangiectasia type 2, various white dot syndromes and other uveitic processes, and some choroidal tumors.

Drusen[17]

Drusen are a hallmark of age-related macular degeneration. On histopathology, nodular drusen appear as eosinophilic dome-shaped structures situated between Bruch's membrane and the displaced, attenuated RPE overlying the drusen.

Hard exudates[18]

Hard exudates are defined as discrete white-yellow lipid depositing in the posterior pole. Hard exudates can be seen in any conditions that are associated with chronic vascular leakage.

Cotton wool spots[19]

Cotton wool spots are defined as localized, white-yellowish, fluffy areas of nerve fiber layer edema due to focal ischemia that causes axoplasmic flow interruption and drainage of axoplasmic content into the retina.

Microaneurysm[20]22

Microaneurysms are a small widening of capillary walls with approximate dimensions of between 10 and 100 μm. In colored fundal images, they appear as round, red spots.

Intraretinal hemorrhage[21,22]

Intraretinal hemorrhage is defined as hemorrhage happens in the retina. Feather- or flame-shaped hemorrhages lie in the superficial capillary plexus. Dot and blot hemorrhage lie deeper in the retina, with blood usually accumulating in the outer plexiform or inner nuclear layers.

Subretinal hemorrhage[23]

Subretinal hemorrhage is defined as hemorrhage is situated deep to the retinal vessels and located under the retinal neurosensory level or retinal pigmented epithelium and appears as dark-red, amorphous hemorrhages.

Preretinal hemorrhage [24]

Preretinal hemorrhage is defined as hemorrhage occur either in the level of subhyaloid space between posterior vitreous face and retina or under internal limiting membrane. Horizontal blood level or boat-shaped hemorrhage is usually apparent, which obscures the underlying retina.

Serous retinal detachment [25]

Serous retinal detachment is defined as the accumulation of fluid in the subretinal space between the sensory retina and the retinal pigmented epithelium resulting in retinal detachment.

Epiretinal membrane[26]

An epiretinal membrane is a fibrocellular tissue found on the inner surface of the retina. It is semi-translucent and proliferates on the surface of the internal limiting membrane.

Macular holes[27]

A macular hole is a small retinal break (full thickness or lamellar) in the macula with a crimson circle appearance 1/4 to 1/2 PD in size.

Optic disc edema[28]

Optic disc edema is used to designate disc swelling lends itself to confusion. It suggests axonal swelling and increased fluid surrounding the axons.

Optic disc pallor[29]

A pale yellow discoloration of the optic disk (the area of the optic nerve head in the retina). The optic disc normally has a pinkish hue with a central yellowish depression.

Increased cup-to-disc ratio[30]

An elevation in the ratio of the diameter of the cup of the optic disc to the total diameter of the disc. An increased cup to disc ratio of over 0.3 may indicate a decrease in the quantity of healthy neuroretinal cells.

Retinal tears[31]

Retinal tears are full thickness breaks in the neurosensory retina that occur secondary to vitreo-retinal traction, including round holes with operculum and horseshoe tears.

Reference

1. Zhang J, Tang FY, Cheung C, Chen X, Chen H. Different effect of media opacity on automated and manual measurement of foveal avascular zone of optical coherence tomography angiographies. Br J Ophthalmol. 2021 Jun;105(6):812-818.
2. Yasser M. Elshatory. Age-Related Macular Degeneration. November 2, 2021. https://eyewiki.org/Age-Related_Macular_Degeneration.
3. Musa Abdelaziz, Mahdi Rostamizadeh, Baseer Ahmad. Branch Retinal Vein Occlusion. January 24, 2022. https://eyewiki.org/Branch_Retinal_Vein_Occlusion
4. Francesco Pichi. Central retinal vein occlusion. April 23, 2022. https://eyewiki.org/Central_Retinal_Vein_Occlusion
5. Cindy W. Mi, Dong Won Lee, Jing Sun, et.al. Central Serous Chorioretinopathy. April 19, 2021. https://eyewiki.org/Central_Serous_Chorioretinopathy#cite_note-:2-2.
6. Liew G, Quin G, Gillies M, Fraser-Bell S. Central serous chorioretinopathy: a review of epidemiology and pathophysiology. Clin Experiment Ophthalmol. 2013;41(2):201-214.

7. Judy E. Kim. Diabetic retinopathy. November 28, 2021. https://eyewiki.org/Diabetic_Retinopathy
8. Omesh P. Gupta. Epiretinal Membrane. December 1, 2021. https://eyewiki.org/Epiretinal_Membrane
9. Omesh P. Gupta. Macular hole. August 7, 2021. https://eyewiki.org/Macular_Hole
10. Fernanda Maria Vaz, Maria Picoto Passarinho. Horseshoe or Flap Tear. April 24, 2022. https://eyewiki.org/Horseshoe_or_Flap_Tear
11. Spraul CW, Grossniklaus HE. Vitreous Hemorrhage. Surv Ophthalmol. 1997 Jul-Aug;42(1):3-39.
12. Sayjal J. Patel. Retinal Detachment. June 18, 2021. https://eyewiki.aao.org/Retinal_Detachment
13. Van Stavern GP. Optic disc edema. Semin Neurol. 2007 Jul;27(3):233-43.
14. Edmond J. FitzGibbon, Sydney Wendt. Optic atrophy. January 29, 2022. https://eyewiki.aao.org/Optic_Atrophy
15. Hollands H, Johnson D, Hollands S, Simel DL, Jinapriya D, Sharma S. Do findings on routine examination identify patients at risk for primary open-angle glaucoma? The rational clinical examination systematic review. JAMA. 2013 May 15;309(19):2035-42.
16. Green W.R. 1996. Ophthalmic Pathology, Volume 2, Chapter 9-Retina, pp 982-1047 W.B. Saunders Company.
17. Andrea Tamine Hoyos Dumar, Juan.David.Arias. Choroidal Neovascularization: OCT Angiography Findings. December 19, 2021. https://eyewiki.org/Choroidal_Neovascularization:_OCT_Angiography_Findings
18. Aliaa Hamed Abdelhakim, et. al. Digital Reference of Ophthalmology - Hard exudates. https://www.columbiaeye.org/education/digital-reference-of-ophthalmology/vitreous-retina/retinal-vascular-diseases/hard-exudates.
19. Aliaa Hamed Abdelhakim, et. al. Digital Reference of Ophthalmology - Cotton wool spots. https://www.columbiaeye.org/education/digital-reference-of-ophthalmology/vitreous-retina/retinal-vascular-diseases/cotton-wool-spots
20. Triwijoyo BK, Sabarguna BS, Budiharto W, Abdurachman E. 2 - Deep learning approach for classification of eye diseases based on color fundus images. In: El-Baz AS, Suri JS, editors. Diabetes and Fundus OCT: Elsevier; 2020. p 25-57.
21. Aliaa Hamed Abdelhakim, et. al. Digital Reference of Ophthalmology - subretinal Hemorrhage. https://www.columbiaeye.org/education/digital-reference-of-ophthalmology/vitreous-retina/retinal-vascular-diseases/dot-and-blot-hemorrhage
22. Aliaa Hamed Abdelhakim, et. al. Digital Reference of Ophthalmology - Flame-shaped Hemorrhage. https://www.columbiaeye.org/education/digital-reference-of-ophthalmology/vitreous-retina/retinal-vascular-diseases/flame-shaped-hemorrhage
23. Aliaa Hamed Abdelhakim, et. al. Digital Reference of Ophthalmology - Dot and Blot Hemorrhage. https://www.columbiaeye.org/education/digital-reference-of-ophthalmology/vitreous-retina/retinal-vascular-diseases/subretinal-hemorrhage
24. Aliaa Hamed Abdelhakim, et. al. Digital Reference of Ophthalmology - Preretinal Hemorrhage. https://www.columbiaeye.org/education/digital-reference-of-ophthalmology/vitreous-retina/retinal-vascular-diseases/preretinal-hemorrhage
25. Joel Epling, Kevin E Lai. Exudative Retinal Detachment. https://eyewiki.aao.org/Exudative_Retinal_Detachment#:~:text=%20Exudative%20Retinal%20Detachment%20%201%20Disease%20Entity.,which%20are%20treated%20surgically%2C%20ERD%20is...%20More%20

26. Omesh P. Gupta. Epiretinal Membrane. December 1, 2021. https://eyewiki.org/Epiretinal_Membrane
27. Sjaarda RN. Macular hole. Int Ophthalmol Clin 1995; 35 (4): 105 22.
28. Van Stavern GP. Optic disc edema. Semin Neurol. 2007 Jul;27(3):233-43.
29. Edmond J. FitzGibbon, Sydney Wendt. Optic atrophy. January 29, 2022. https://eyewiki.aao.org/Optic_Atrophy
30. Sebastian Köhler, Michael Gargano, Nicolas Matentzoglu, et.al. The Human Phenotype Ontology in 2021, Nucleic Acids Research, Volume 49, Issue D1, 8 January 2021, Pages D1207–D1217
31. Fernanda Maria Vaz, Maria Picoto Passarinho. Horseshoe or Flap Tear. April 24, 2022. https://eyewiki.org/Horseshoe_or_Flap_Tear

Supplementary Text S2. Detailed annotation process

The labelling team consisting of 2 junior ophthalmologists (JO) with more than 3 years of clinical experience, 2 senior ophthalmologists (SO) with more than 6 years of clinical experience and 1 specialized ophthalmologist with more than 20 years of clinical experience was divided into 2 groups which consisted of 1 JO and 1 SO and the datasets were divided into 2 labelling quarters randomly and equally. Each quarter were firstly labelled by the JO and checked by the SO. The divergences were finally confirmed by the specialized ophthalmologist. The annotation workflow consisted of 2 parts: (1) The images with incomplete view of the retina due to VH, RMO (vitreous opacity, cataract, asteroid hyalosis, etc.) and RD were firstly divided into pathological poor-quality images group with disease labels. (2) The pathological lesions were labelled using bounding boxed using LabelImg software (1.8.1) and the classification labels, pathological changes and anatomy location were recorded. The lesions in the adjacent region were boxed together if they belonged to the same type.

Supplementary Text S3. Preprocessing of images

UWF images were processed by contrast limited adaptive histogram equalization (CLAHE) before being fed into the CAFPN. Because most lesions are much smaller than the UWF size, processed image were separated into tiles of 256*256 during test. To further improve the recognition of small lesions like tiny hemorrhages and deposits, UWFs were divided into patches of 128*128 and unsampled to 256*256 during training. Meanwhile, focal loss with α=0.3 and γ=1.5 was adopted as loss function to achieve the right balance between positives and negatives.

Supplementary Text S4. Detailed training process of the mass screening system

The training process is as follows:

Assume the AdaBoost SVM $M = \{M_1, M_2, \cdots, M_N\}$, training set $\{(x_i, y_i), i \in \{1, 2, \cdots, I\}\}$,where $y_i = [y_{i1}, y_{i1}, \cdots, y_{iJ}]$, $y_{ij} \in \{0, 1\}$ is the label array of J diseases, the inference $\hat{y}_i$ of x_i output from M was formulated as

$$\hat{y}_i = \sum_{n=1}^{N} w_n \cdot M_n(x_i).$$

1. Initializing N SVM model $\{M_1, M_2, \cdots, M_N\}$;
2. Initializing sample weights $D_1 = (d_{11}, d_{12}, \cdots, d_{1I}), d_{1i} = 1/I$;

For training model M_n,

3. Training M_n in training set with sample weights D_n, computing its error of each disease

$$e_{nj} = P\left(M_{nj} \neq y_j\right) = \sum_i d_{mi} \cdot I(M_{nj} \neq y_j);$$

4. Calculating average error $e_n = \frac{1}{J}\sum_j e_{nj}$ and M_n's inference weight

$$w_n = \frac{1}{2}\ln\left(\frac{1-e_n}{e_n}\right);$$

5. Updating sample weights $D_{n+1} = \left(d_{n+1,1}, d_{n+1,2}, \cdots, d_{n+1,I}\right)$, where

$$d_{n+1,i} = \frac{d_{ni} \cdot \exp\left(-w_n \cdot M_n(x_i)\right)}{\sum_i d_{ni} \cdot \exp\left(-w_n \cdot M_n(x_i)\right)}$$

6. Back to step 3, training M_{n+1} and D_{n+1} until all N models were trained.

Since CRVO and BRVO do not coexist, we add a penalty term P to the loss function L, as follows:

$$L = L_{cls} + P,$$

$$L_{cls} = \sum_{j=1}^{J} L_j,$$

$$L_j = \begin{cases} -y_j \cdot \log\left(\hat{y}_j\right) \\ -\left(1 - y_j\right) \cdot \log\left(1 - \hat{y}_j\right) \end{cases},$$

$$P = -\lambda \sum_t y_t \cdot \log\left(\frac{\exp(\hat{y}_t)}{\sum_t \exp(\hat{y}_t)}\right),$$

where $t \in$ {CRVO, BRVO, neither CRVO or BRVO} and y_t is the one-hot label of BRVO and CRVO. In this paper, model number N was set to 50, the disease number J was eight including DR, AMD, CRVO, BRVO, CSCR, MH, EMM and RT.

Supplementary Text S5. Detailed evaluation results of modules in IEDSS

IEDSS was based on the four modules and we evaluated the performance of the preliminary screening module and lesion atlas mapping module separately to make sure IEDSS was reliable. IEDSS first screened the diseases reducing image quality using the preliminary screening module. The confusion matrix was presented in Supplementary Figure S1a - S1c. The preliminary screening module exhibited good performance in identifying VH, RD and RMO with ACCs over 0·993 and F1 scores over 0·933. The sensitivities and the specificities reached over 0·941 and 0·994 (Table 2).

The performance of lesion atlas mapping module was then assessed. The diverse lesions could be correctly detected with average precision ranging from 0·745 to 0·927 (Supplementary Figure S2). The module performed better in recognizing well-circumscribed objects such as MH and PRH. For lesions in ONH region that couldn't coexist, a multi-class model was constructed, with F1 scores over 0·929, ACCs over 0·992, sensitivities over 0.940 and specificities over 0·995 (Table 2). The confusion matrix was described in Supplementary Figure S1d - S1f.

Table S1 The distribution of multimorbidity dataset in SAHZU

	Number (%)	Total no· of eyes		No· of patients (male : female)	Age, mean ± SD
		Right	Left		
Glaucoma + DR	120 (24%)	65	55	116 (70 : 46)	61·92 ± 13·42
Glaucoma + BRVO	90 (18%)	51	39	90 (38 : 52)	60·87 ± 11·04
Glaucoma + CRVO	68 (13·6%)	30	38	64 (29 : 35)	66·46 ± 13·23
BRVO + DR	30 (6%)	22	8	30 (19 : 11)	60·21 ± 9·66
Glaucoma + MH	23 (4·6%)	14	9	23 (14 : 9)	73·00 ± 8·91
AMD + Glaucoma	22 (4·4%)	9	13	19 (11 : 8)	78·42 ± 5·92
AMD+BRVO	18 (3·6%)	10	8	18 (8 : 10)	69·86 ± 11·77
CRVO + DR	18 (3·6%)	7	11	16 (7 : 9)	74·50 ± 4·55
Glaucoma + CSCR	18 (3·6%)	7	11	16 (10 : 6)	55·70 ± 14·75
BRVO+CSCR	15 (3%)	11	4	13 (9 : 4)	52·64 ± 11·69
AMD + DR	13 (2·6%)	8	5	12 (8 : 4)	67·47 ± 5·54
BRVO + MH	12 (2·4%)	4	8	10 (6 : 4)	60·5 ± 7·64
DR+MH	9 (1·8%)	3	6	7 (3 : 4)	63·79 ± 10·41
CSCR+EMM	8 (1·6%)	5	3	8 (5 : 3)	50·79 ± 9·30
CRVO+CSCR	6 (1·2%)	4	2	5 (3 : 2)	68·17 ± 9·40
AMD+MH	6 (1·2%)	4	2	6 (3 : 3)	58·11 ± 5·56
BRVO + EMM	6 (1·2%)	4	2	6 (2 : 4)	68·16 ± 12·16
CRVO + MH	5 (1%)	3	2	5 (1 : 4)	78·67 ± 11·93
CRVO+OA	5 (1%)	3	2	5 (4 : 1)	73·67 ± 4·63
CSCR+MH	4 (0·8%)	1	3	4 (2 : 2)	56·21 ± 7·74
BRVO+OA	4 (0·8%)	3	1	3 (2 : 1)	69·33 ± 1·58
Total	500	268	232	476	63·58 ± 12·65

SAHZU, the Second Affiliated Hospital of Zhejiang University, School of Medicine ; DR, diabetic retinopathy; CSCR, central serous chorioretinopathy; AMD, age -related macular degeneration; MH, macular Hole; EMM, epimacular membrane; CRVO, central retinal ve in occlusion; BRVO, branch retinal vein occlusion; OA, optic atrophy.

Table S2 The comparison test between Interpretable Eye Diseases Screening System (IEDSS) and human ophthalmologists in the internal dataset

	IEDSS			Junior ophthalmologist			Senior ophthalmologist		
	ACC (%) (95%CI)	Sensitivity (%) (95% CI)	Specificity (%) (95% CI)	ACC (%)	Sensitivity (%)	Specificity (%)	ACC (%)	Sensitivity (%)	Specificity (%)
wet-AMD	95·34(94·63-96·06)	95·49(92·22-97·47)	95·33(94·50-96·04)	73·96	69·61	98·68	86·46	81·64	99·60
BRVO	97·55(97·02-98·08)	97·82(94·70-99·19)	97·53(96·90-98·04)	93·89	93·89	99·29	97·38	97·38	99·81
CRVO	94·25(93·46-95·05)	98·14(94·22-99·52)	94·06(93·16-94·84)	91·93	91·93	98·22	96·89	96·89	99·71
CSCR	95·68(94·98-96·37)	89·23(83·80-93·06)	96·08(95·32-96·72)	68·21	58·33	97·81	86·15	81·16	99·04
DR	96·07(95·41-96·73)	95·91(94·56-96·95)	96·15(95·23-96·91)	90·78	90·16	98·28	98·43	98·43	99·49
EMM	97·67(97·16-98·19)	94·75(91·45-96·87)	97·97(97·38-98·43)	82·3	74·26	99·7	89·18	82·93	99·77
MH	99·09(98·77-99·42)	98·61(94·56-99·76)	99·11(98·70-99·40)	95·14	90·73	100·00	98·61	97·26	100·00
RT	96·73(96·13-97·34)	96·50(94·17-97·96)	96·77(96·04-97·37)	85·78	75·1	100·00	97·44	95	100·00
VH	99·39(99·16-99·61)	97·03(93·35-98·79)	99·49(99·14-99·69)	98·02	98·02	99·71	99·51	99·5	100·00
RD	99·65(99·48-99·82)	99·17(98·22-99·64)	99·76(99·44-99·90)	98·81	97·66	100·00	99·88	99·76	100
RMO	99·46(99·24-99·67)	94·17(89·80-96·82)	99·71(99·43-99·86)	94·66	91·12	99·62	98·54	97·13	99·9
ODE	99·52(99·28-99·75)	100·00(95·60-100·00)	99·50(99·17-99·70)	94·29	89·19	100·00	98·10	96·26	100·00
OA	99·73(99·55-99·91)	97·98(92·19-99·65)	99·78(99·53-99·90)	90·91	83·33	100·00	96·97	94·12	100·00
SG	99·24(98·95-99·54)	94·06(89·60-96·75)	99·58(99·26-99·77)	86·14	75·65	100	92·08	85·32	100

DR, diabetic retinopathy; CSCR, central serous chorioretinopathy; wet -AMD, wet age-related macular degeneration; MH, macular Hole; EMM, epimacular membrane; CRVO, central retinal vein occlusion; BRVO, branch retinal vein occlusion; RT, retinal tears; ODE, optic disc edema; OA, optic atrophy; SG, suspected glaucoma; RD, retinal detachment; VH, vitreous hemorrhage; RMO, refractive media opacity; ACC, accuracy.

Table S3 The comparison of precision between Interpretable Eye Diseases Screening System (IEDSS) and classic models

	IEDSS			Multi-class ResNetXt-50	Multi-label ResNetXt-50	Multi-label ViT	CAFPN+SVM
	SAHZU	APHNU	FAHUSTC				
wet-AMD	66·11(60·46-71·33)	41·32(30·73-52·77)	67·56(61·04-73·46)	37·91(32·50-43·64)	53·20(47·43-58·88)	51·24(45·49-56·96)	53·14(47·37-58·82)
BRVO	74·67(68·66-79·86)	67·63(58·82-75·34)	85·34(80·27-89·28)	50·00(43·58-56·42)	62·99(56·57-68·98)	70·68(64·49-76·2)	61·93(55·50-67·97)
CRVO	45·80(38·29-53·50)	35·54(28·00-43·88)	43·01(35·64-50·71)	46·72(39·18-54·41)	31·42(24·76-38·95)	29·39(22·9-36·84)	35·24(28·28-42·88)
CSCR	58·78(51·77-65·46)	58·90(44·97-71·54)	36·45(26·91-47·19)	27·44(21·66-34·09)	36·60(30·16-43·56)	39·19(32·61-46·19)	47·50(40·61-54·49)
DR	93·00(91·38-94·34)	91·51(89·43-93·21)	94·89(93·36-96·07)	78·34(75·87-80·62)	85·57(83·42-87·49)	82·63(80·33-84·71)	86·68(84·59-88·52)
EMM	82·57(77·92-86·42)	43·75(34·69-53·25)	40·36(32·75-48·47)	45·06(39·57-50·67)	64·37(58·84-69·53)	54·2(48·59-59·7)	60·33(54·74-65·66)
MH	83·53(76·62-88·70)	58·23(44·18-71·06)	63·64(50·77-74·81)	54·55(46·40-62·45)	60·56(52·41-68·17)	65·87(57·8-73·11)	77·53(70·05-83·58)
RT	81·66(77·72-85·03)	69·15(62·69-74·94)	68·52(62·40-74·05)	73·42(69·04-77·38)	68·93(64·40-73·12)	64·65(60·01-69·02)	70·34(65·85-74·46)
VH	89·91(84·98-93·35)	93·90(89·78-96·42)	95·60(92·72-97·37)	61·94(55·08-68·35)	NA	NA	NA
RD	98·93(97·99-99·44)	98·10(96·11-99·08)	98·69(97·32-99·37)	88·35(86·01-90·35)	NA	NA	NA
RMO	93·72(89·54-96·30)	88·39(80·74-93·26)	84·67(77·30-89·96)	54·87(48·04-61·51)	NA	NA	NA
ODE	86·78(78·98-91·97)	84·44(70·07-92·64)	86·96(76·38-93·22)	32·77(24·54-42·22)	NA	NA	NA
OA	93·27(86·55-96·76)	87·01(77·01-93·06)	88·10(78·93-93·60)	23·96(16·62-33·23)	NA	NA	NA
SG	93·60(89·34-96·22)	86·49(81·45-90·32)	85·42(81·72-88·47)	25·94(20·38-32·39)	NA	NA	NA

The multi-label models including Multilabel ResNetXt-50, Multi-label Vit and CAFPN+SVM were not tested on the multi-class labels, including VH, RD, RMO, ODE, OA, SG.

DR, diabetic retinopathy; CSCR, central serous chorioretinopathy; wet-AMD, wet age-related macular degeneration; MH, macular Hole; EMM, epimacular membrane CRVO, central retinal vein occlusion; BRVO, branch retinal vein occlusion; RT, retinal tears; ODE, optic disc edema; OA, optic atrophy; SG, suspected glaucoma; RD, retinal detachment; VH, vitreous hemorrhage; RMO, refractive media opacity; NA, not applicable.

Table S4 The sensitivity and specificity of comparison experiment between Interpretable Eye Diseases Screening System (IEDSS) and classic algorithms

	Multi-class ResNetXt-50		Multi-label ResNetXt-50		Multi-label ViT		CAFPN+SVM		IEDSS	
	Sensitivity (%) (95% CI)	Specificity (%) (95% CI)	Sensitivity (%) (95% CI)	Specificity (%) (95% CI)	Sensitivity (%) (95% CI)	Specificity (%) (95% CI)	Sensitivity (%) (95% CI)	Specificity (%) (95% CI)	Sensitivity (%) (95% CI)	Specificity (%) (95% CI)
wet-AMD	75·69(70·42-80·29)	91·64(90·77-92·43)	75·00(69·69-79·65)	93·71(92·78-94·52)	85·76(81·26-89·33)	92·22(91·21-93·12)	88·19(83·96-91·43)	92·58(91·59-93·46)	95·49(92·22-97·47)	95·33(94·50-96·04)
BRVO	93·45(89·48-95·99)	95·06(94·37-95·66)	92·14(87·92-94·97)	95·97(95·22-96·61)	94·76(91·07-96·98)	97·08(96·42-97·62)	95·20(91·60-97·3)	95·65(94·87-96·31)	97·82(94·70-99·19)	97·53(96·90-98·04)
CRVO	75·16(67·95-81·19)	96·86(96·30-97·34)	85·09(78·78-89·77)	90·50(89·42-91·47)	86·34(80·18-90·80)	89·38(88·26-90·41)	88·20(82·30-92·31)	91·70(90·69-92·62)	98·14(94·22-99·52)	94·06(93·16-94·84)
CSCR	53·33(46·33-60·2)	93·70(92·94-94·38)	70·77(64·03-76·70)	92·32(91·33-93·2)	69·74(62·97-75·76)	93·22(92·28-94·05)	77·95(71·62-83·20)	94·60(93·75-95·34)	89·23(83·80-93·06)	96·08(95·32-96·72)
DR	71·39(68·71-73·93)	93·34(92·45-94·13)	83·04(80·77-85·10)	92·54(91·35-93·57)	81·91(79·58-84·03)	90·82(89·53-91·97)	89·39(87·48-91·04)	92·68(91·50-93·70)	95·91(94·56-96·95)	96·15(95·23-96·91)
EMM	71·80(66·51-76·56)	93·72(92·95-94·41)	73·44(68·22-78·09)	95·87(95·10-96·52)	74·10(68·9-78·69)	93·64(92·71-94·46)	84·26(79·75-87·92)	94·37(93·49-95·14)	94·75(91·45-96·87)	97·97(97·38-98·43)
MH	87·50(81·11-91·94)	97·62(97·13-98·03)	89·58(83·52-93·59)	97·34(96·72-97·85)	95·14(90·31-97·63)	97·76(97·18-98·22)	95·83(91·21-98·08)	98·74(98·28-99·07)	98·61(94·56-99·76)	99·11(98·70-99·40)
RT	81·12(77·15-84·54)	96·95(96·38-97·43)	85·31(81·65-88·35)	94·27(93·36-95·06)	92·07(89·13-94·27)	92·49(91·47-93·4)	92·31(89·39-94·47)	94·20(93·28-94·99)	96·50(94·17-97·96)	96·77(96·04-97·37)
VH	95·05(91·13-97·29)	97·29(96·77-97·73)	NA	NA	NA	NA	NA	NA	97·03(93·35-98·79)	99·49(99·14-99·69)
RD	98·10(96·94-98·83)	97·07(96·47-97·56)	NA	NA	NA	NA	NA	NA	99·17(98·22-99·64)	99·76(99·44-99·90)
RMO	90·29(85·48-93·63)	96·48(95·89-96·99)	NA	NA	NA	NA	NA	NA	94·17(89·80-96·82)	99·71(99·43-99·86)
ODE	92·38(85·68-96·09)	95·53(94·88-96·1)	NA	NA	NA	NA	NA	NA	100·00(95·60-100·00)	99·50(99·17-99·70)
OA	86·87(78·82-92·16)	93·88(93·14-94·54)	NA	NA	NA	NA	NA	NA	97·98(92·19-99·65)	99·78(99·53-99·90)
SG	75·25(68·86-80·69)	90·04(89·11-90·89)	NA	NA	NA	NA	NA	NA	94·06(89·60-96·75)	99·58(99·26-99·77)

The multi-label models including Multi-label ResNetXt-50, Multi-label ViT and CAFPN+SVM were not tested on the multi-class labels, including VH, RD, RMO, ODE, OA, SG.

DR, diabetic retinopathy; CSCR, central serous chorioretinopathy; wet-AMD, wet age-related macular degeneration; MH, macular Hole; EMM, epimacular membrane; CRVO, central retinal vein occlusion; BRVO, branch retinal vein occlusion; RT, retinal tears; ODE, optic disc edema; OA, optic atrophy; SG, suspect ed glaucoma; RD, retinal detachment; VH, vitreous hemorrhage; RMO, refractive media opacity; NA, not applicable.

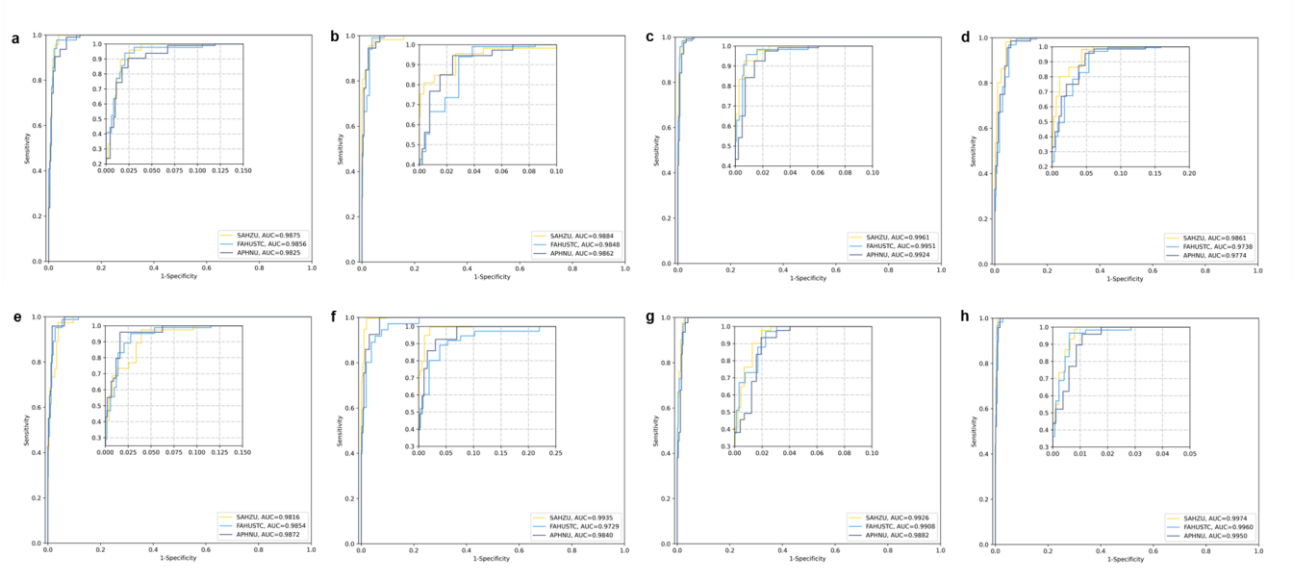

Supplementary Figure S1. The receiver operating characteristic curve of the mass screening model in identifying diabetic retinopathy (a), wet age-related macular degeneration (b), branch retinal vein occlusion (c), central retinal vein occlusion (d), central serous chorioretinopathy (e), epimacular membrane (f), retinal tears (g), macular holes (h) in the Second Affiliated Hospital of Zhejiang University, School of Medicine (SAHZU), the Affiliated People's Hospital of Ningbo University (APHNU) and the First Affiliated Hospital of University of Science and Technology of China (FAHUSTC).

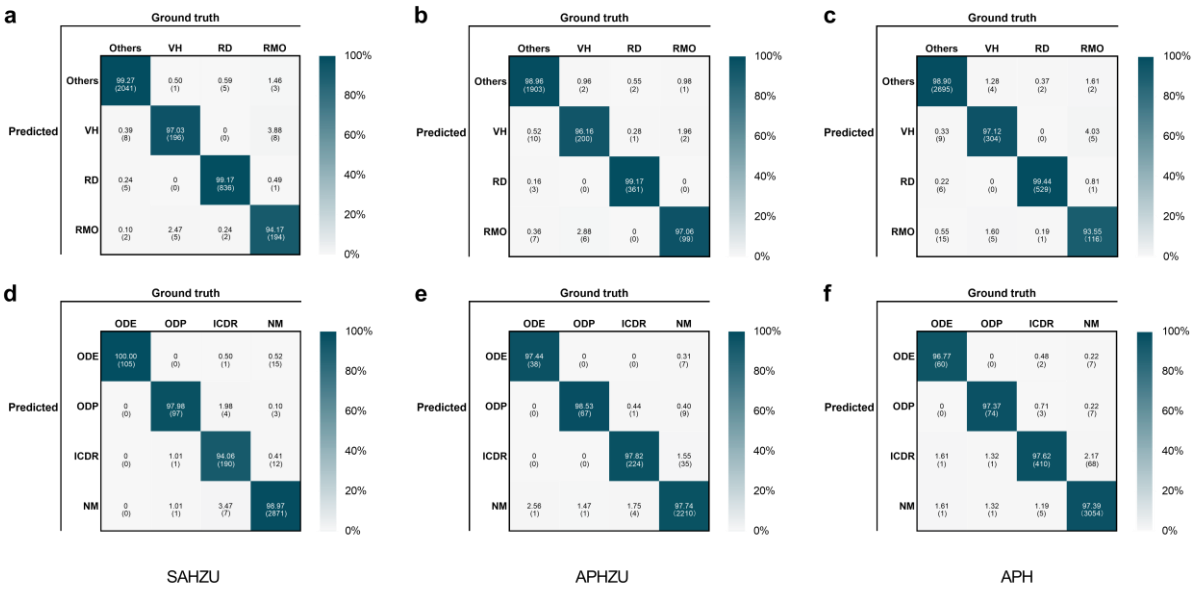

Supplementary Figure S2. The confusion matrix of preliminary screening module (a-c) and multi-class model identifying lesions in optic disc region (d-f) in the Second Affiliated Hospital of Zhejiang University, School of Medicine (SAHZU), the Affiliated People's Hospital of Ningbo University (APHNU) and the the First Affiliated Hospital of University of Science and Technology of China (FAHUSTC).

ODE, optic disc edema; ODP, optic disc pallor; ICDR, increased cup-to-disc ratio; RD, retinal detachment; VH, vitreous hemorrhage; RMO, refractive media opacity.

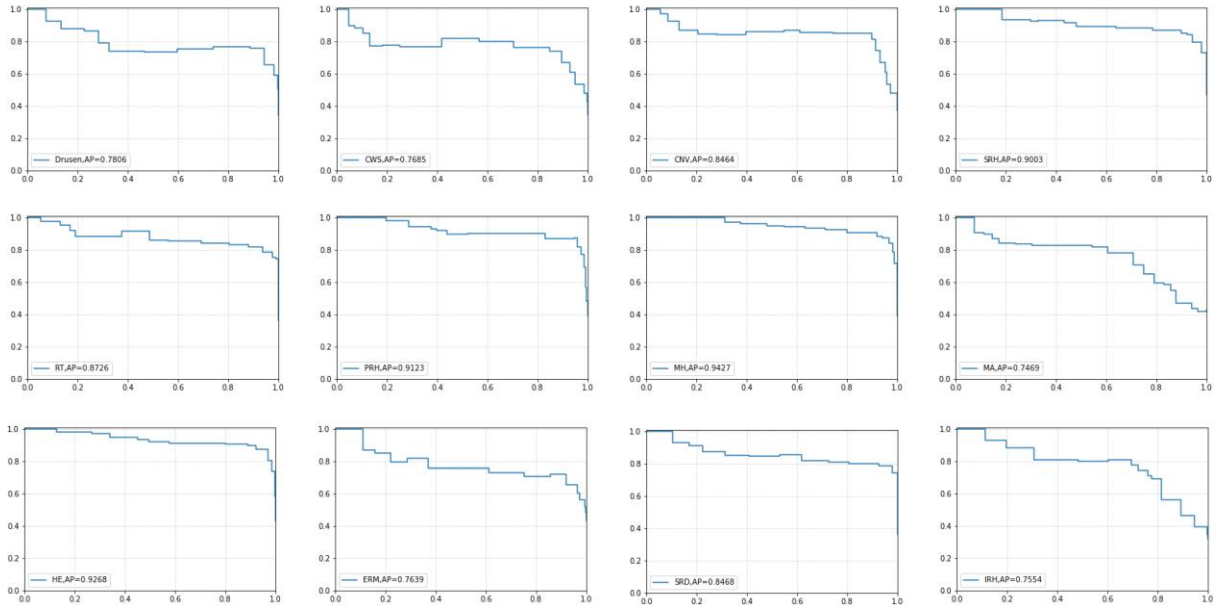

Supplementary Figure S3. The precision-recall curve of the lesion atlas mapping model in detecting and locating 12 classes of lesions.
CNV, choroidal neovascularization; HE, hard exudates; CWS, cotton wool spots; MA, microaneurysm; IRH, intraretinal hemorrhage; SRH, subretinal hemorrhage; PRH, preretinal hemorrhage; SRD, serous retinal detachment; ERM, epiretinal membrane; MH, macular holes; RT, retinal tears.

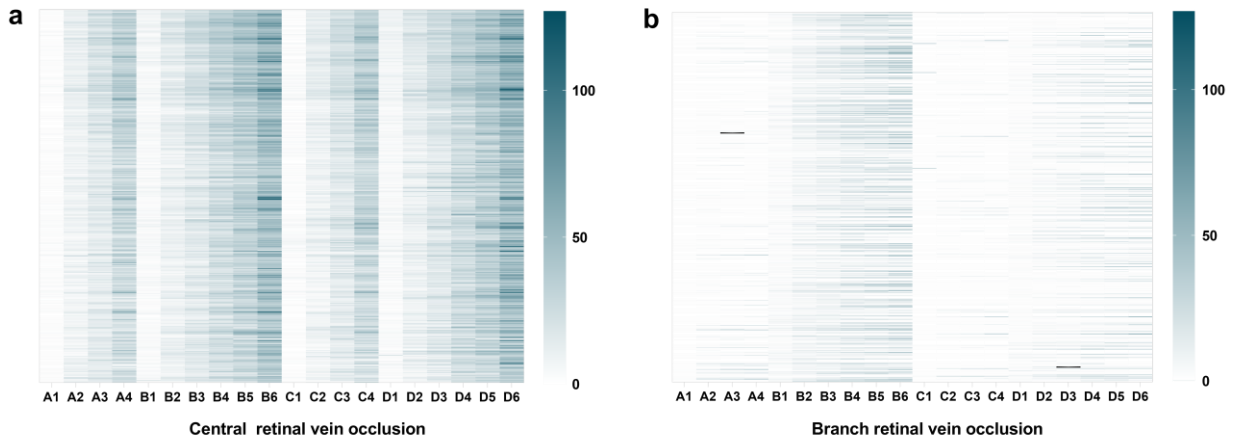

Supplementary Figure S4. The detailed heatmap demonstrating intraretinal hemorrhage in each subject of central retinal vein occlusion (a) and branch retinal vein occlusion (b). The diversity of pathological and anatomical distribution could be clearly found in the heatmap.

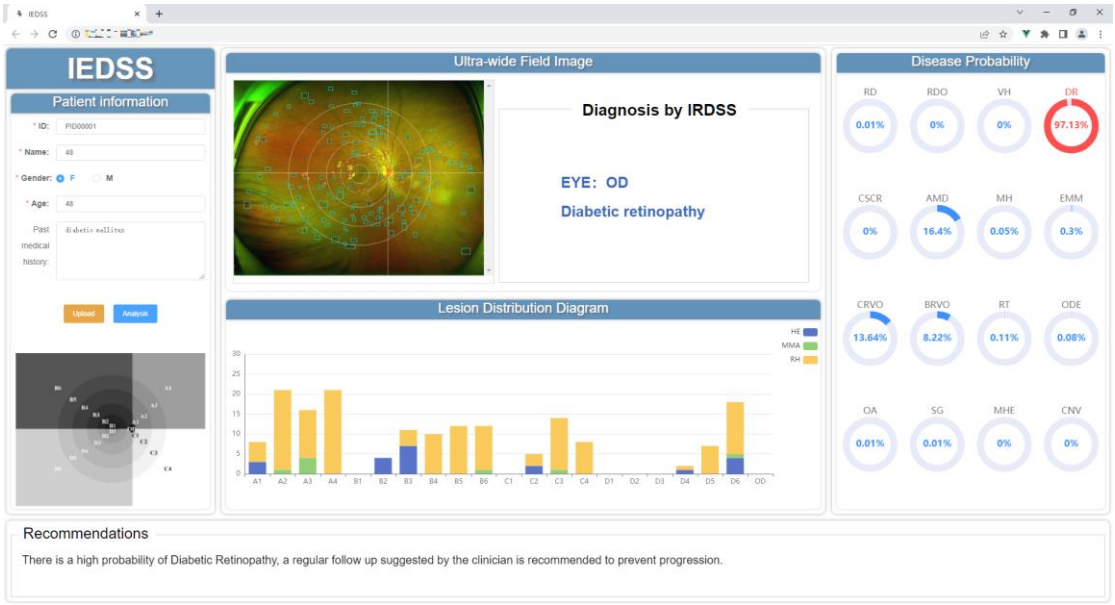

Supplementary Figure S5. The cloud platform interface of Interpretable eye diseases screening system (IEDSS). Clinicians could read the probability of different diseases, the diagnostic basis and the referral recommendations from the interface. They could combine the results of IEDSS and their clinical experience to make a more reasonable judgement.